Peculiarities in the transfer of a repetitively pulsed CO_2 laser radiation through the atmosphere

V.M. Osipov, I.A. Popov, and Yu.A. Rezunkov

Scientific Research Institute for Complex Testing of Opto-Electronic Devices and Systems, Sosnovyi Bor, Leningrad Region

Received March 6, 2000

Interaction between the radiation of 30-kW repetitively pulsed CO_2 laser and air has been studied both theoretically and experimentally. Based on the results of these studies, the peculiarities of the interaction have been considered, which are significant in solving the problems on precisely delivering of laser energy to remote objects.

Introduction

At present there are some promising research problems called by the need in precisely transferring high-power laser radiation through the atmosphere at very long distances. These problems include energy transfer to orbiting stations, destruction of space debris, initiation of lightning discharges, development of laser reaction-plasma engines, etc. In particular, the idea of using laser radiation to launch spacecraft is very interesting. The propulsion of such a spacecraft is produced by the shock wave generated at optical breakdown of a working gas in the area of focusing of a high-power laser beam transferred to the spacecraft. As was estimated by the authors of one of such projects,[1] to launch a satellite having the mass of 120 kg using a repetitively pulsed CO_2 laser, the laser radiation power should be at the level of 100 MW.

The problem of efficient transfer of laser radiation with the needed characteristics through the atmosphere within a diffraction-limited spatial angle is one of the main factors determining the possibility of solving the above-mentioned problems, in particular, the problem of launching spacecraft.

The most significant processes affecting the characteristics of high-power laser radiation during its propagation through the atmosphere are known rather well. They include radiation extinction by atmospheric gases and atmospheric aerosols, thermal blooming, radiation scattering at turbulent inhomogeneities of the atmosphere, and some other nonlinear effects. Generally speaking, one or another method can be found to describe each of these processes and the corresponding estimates of its influence on laser beam characteristics can be obtained. However, the complexity of the problem is determined by the following. First, there are some peculiarities in high-power laser radiation that restrict the use of the numerical estimates of the effects of radiation interaction with the atmosphere. Second, one needs to take into account the joint effect of many factors influencing the interaction.

The interaction of radiation with the atmosphere is mostly determined by the characteristics of the laser radiation itself (wavelength, laser operating mode: continuous wave or repetitively pulsed, mean and pulse power, pulse repetition frequency, etc.). Therefore, for understanding the processes of interaction of high-power laser radiation with the atmosphere, complex experimental studies of these processes for particular lasers under atmospheric conditions are very important. In this paper, we consider the peculiarities of transfer of radiation of high-power repetitively pulsed electroionization CO2 laser through the atmosphere. Experiments were conducted along a near-ground atmospheric path about 3 km long. The optical axis of the laser beam was 3 to 4 m above the ground, the power of the radiation varied from 3.4 to 30 kW, the total energy emitted by a laser in a session was from 3 to 42 kJ, and the pulse repetition frequency was from 20 to 200 Hz.

The results of these studies have been considered in detail in Refs. 2–4. This paper briefly reviews these results as applied to the above mentioned problems and considers some peculiarities of interaction, which can play a principal role in transfer of the radiant energy to the top of the atmosphere.

1. Extinction of CO_2-laser radiation by atmospheric gases and aerosols

The radiation emitted by a high-power CO_2 laser is, as a rule, partially coherent with a complex spectral shape of a pulse. Previous experiments[5] showed, in particular, that the line profile of a repetitively pulsed electroionization CO_2 laser consists of one or several components with the width $2\gamma = 4.7 \cdot 10^{-3}$ cm^{-1} at the level of 0.3 of the maximum intensity, and the separation between the centers of the edge components does not exceed 0.015 cm^{-1}. Besides, it is known that because of the effect of collisional shift, the center of the CO_2-laser line does not coincide with the center of the absorption line of atmospheric CO_2 and the value of this detuning is different at different altitudes.

0235-6880/00/05 402-10 $02.00

To estimate the influence of these effects on the passage of laser radiation through the atmosphere, the following characteristics should be determined: the collisional shift coefficient at the CO_2 10P20 line (at which the lasing occurs) for the case of collision with the molecules of the atmosphere and the collisional shift coefficients at the same line for collisions with molecules of gases that form the active medium of the laser.

Omitting here detailed analysis of the available literature data, let us only note the following circumstances which are significant for the problem under consideration.

Almost all studies of the shift of the CO_2-laser line (except for Ref. 6) were performed at low pressures in active media. The obtained values of the shift coefficients of the laser frequency are low ($\beta \le 0.01$ cm$^{-1} \cdot$ atm^{-1}) and are in agreement with each other. These values are far lower than the values of β obtained in Refs. 7 and 8 by the methods of classic spectroscopy for collisions with molecules in the air under atmospheric pressure and in the above-mentioned Ref. 6 for CO_2–He collisions at a high pressure of the active medium ($P \le 6$ atm).

Such a disagreement between the obtained results can be partially caused by frequency pulling toward the center of the amplification line. In Ref. 9 the frequency pulling was close in value to the collisional shift. However, the main cause, in our opinion, is the dependence of the shift coefficient on the pressure of the gas medium. This is evidenced by the results from Ref. 10, in which it was shown that not only the value of the shift coefficient, but the shift direction as well can be different at different pressure. Thus, the shift coefficient $\beta_{CO_2-CO_2}$ $(1.57 \pm 0.46) \cdot 10^{-3}$ cm$^{-1} \cdot$ atm^{-1} at $P \le (3 - 4) \cdot 10^{-4}$ atm proved to be equal to $-(2 \pm 1.3) \cdot 10^{-3}$ cm$^{-1} \cdot$ atm^{-1} at the pressure about 0.01 atm. Consequently, the shift coefficient should be measured at a pressure as close as possible to the operating conditions of the electroionization CO_2 laser in the atmosphere. Let us present here the results of studies with the instrumentation described in Ref. 8, which allowed fulfillment of the above requirement.

The following values of the shift coefficient at the CO_2 10P20 line were obtained:

– $\beta_{CO_2-air} = 0.005$ cm$^{-1} \cdot$ atm^{-1} for the collisions in air;

– $\beta_{CO_2-N_2-He} = (0.006 \pm 0.002)$ cm$^{-1} \cdot$ atm^{-1} for the case of collision of CO_2 (one part) with nitrogen molecules (two parts) and helium (three parts).

We use these values to estimate the effect of collisional shift and nonmonochromaticity of the laser radiation on the value of molecular absorption as the laser radiation passes through the atmosphere. In accordance with the technique described in Ref. 11, for the transmission $T_{\Delta\nu}$ of the vertical path from the level z_1 to the top of the atmosphere z_2 we have:

$$T_{\Delta\nu} = \int_{\Delta\nu} g(\nu - \nu_0)\, T(\nu)\, d\nu, \qquad (1)$$

$$T_\nu = \exp\left\{ - \int_{z_1}^{z_2} S(z)\, f[\nu - \nu_0', \gamma(z)]\, u(z)\, dz \right\},$$

where $g(\nu - \nu_0)$ is the shape of the laser line with the center at ν_0; S, f, and γ are the intensity, line shape, and halfwidth of the absorption line with the center at ν_0'; $u(z)$ is the content of the absorbing gas.

The results calculated for the midlatitudinal summer are shown in Fig. 1. Curve *1* shows the dependence of the transmission of the vertical path on the altitude of the lower boundary ignoring the collisional shift. The allowance for the shift of the absorption line of atmospheric CO_2 leads to an insignificant change of the transmission function, since the shift occurs within the collisional halfwidth of the line. The influence of the shift of the laser line is more significant (curve *2*), since in the upper atmospheric layers the center of the laser line does not coincide with the center of the narrow absorption line. This effect is somewhat weaker (by about 2–3%), if we take into account the limited width of the laser line, which in our case is 0.004 cm^{-1}. The allowance for the complex structure of the laser line profile (curve *3*) in this case also does not lead to further "clearing-up" of the atmosphere, since the parameters used according to Ref. 5 lead to coincidence of the center of one profile component with the center of the absorption line in the lower atmospheric layers. Nevertheless, in each case the transmission of the vertical path increases by 1.4–1.5 times.

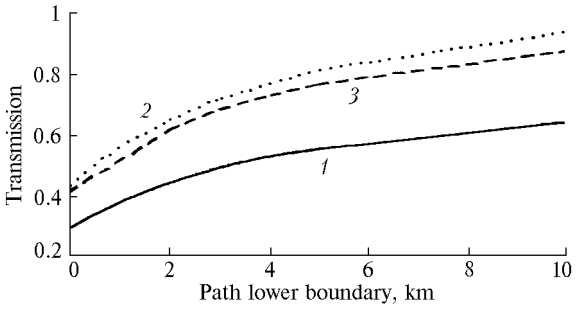

Fig. 1. Transmission of vertical atmospheric path for radiation at 10.6 μm.

As the results of field studies[12,13] on an open-path showed, the characteristics of aerosol absorption K_{ab} and scattering K_{sc} of CO_2-laser radiation in the near-ground atmospheric layer also do not correspond to the used standard models of the atmospheric extinction. Analysis of the experimental data from Ref. 2 on the extinction of radiation under different seasonal and weather conditions showed that at poor visibility the part of aerosol extinction can exceed significantly (by an order of magnitude) the part of molecular absorption. Using the wide variety of empirical and semiempirical models of aerosol extinction available in the literature, we certainly can select the most suitable model to describe the dependence of the aerosol

extinction coefficients K_{ext} on the meteorological visibility range (MVR). Under conditions of good visibility (MVR ≥ 10 km), the closest agreement was obtained with the use of the model of continental aerosol,[14] while the synoptic models gave good agreement in the case of poor visibility.[15]

However, the measurements of the scattering phase function of the CO_2-laser radiation on the open path[13] showed that the scattering coefficient K_{sc} and the relative part of the scattered radiation (K_{sc}/K_{ext}) are far (sometimes by an order of magnitude) less than the values following from the model of Ref. 14. The shape of the measured scattering phase function also differs markedly. It turned out to be far more forward peaked than it had been first supposed based on literature data. In making attempts to use microphysical approach[16] for calculating the aerosol scattering and aerosol extinction coefficients, it turned out that the experimental values of the scattering coefficient are also much lower than the calculated ones. In contrast, the experimental values of the aerosol extinction coefficient K_{ext} are about twice as large as the calculated ones. The results of these measurements and calculations are given in Table 1.

This fact indicates that the values of the real and imaginary parts of the aerosol refractive index at the wavelength of 10.6 μm are likely to be corrected. The noted circumstances should be kept in mind when considering one of the principal mechanisms of nonlinear interaction – the effect of thermal defocusing of laser radiation. The strength of this effect depends on the energy of laser radiation absorbed by the atmosphere and, consequently, on the imaginary part of the aerosol refractive index.

3. Efficiency of delivery of CO_2-laser radiation with power up to 30 kW along atmospheric paths

As high-power laser beam passes through the atmosphere, some nonlinear effects occur and influence the efficiency of radiation transfer. Among these effects, the effect of thermal blooming is known as having one of the lowest threshold. The influence of this effect depends on the time of air heating in the beam propagation channel, the radiation intensity distribution over the beam aperture, and the processes of heat removal from the propagation channel. As repeated laser pulses pass through the atmosphere, the accompanying effects can differ from those in the case of continuous-wave radiation. Besides, the atmospheric turbulence, which leads to broadening of laser beams and random walks of its axis, increases the effective radius of the beam, what also influences the manifestation of the thermal blooming effect.

Therefore, in the experimental studies of the effect of thermal blooming on a near ground atmospheric path,[3] the specialized techniques for direct monitoring of the state of the atmospheric channel of laser beam propagation were used. These techniques provide measurements of aberrations induced by CO_2-laser radiation based on the wave front distortions of the He–Ne-laser radiation propagating along the same path but in the opposite direction. To monitor the wave front distortions of the sensing radiation ($\lambda = 0.63$ μm), two modifications of the Hartmann method with measurement of local tilts of a great number of small areas (subapertures) of the wave surface were used. In the first modification, the aperture of the wave front of the sensing radiation was limited by a diaphragm with a ring-like hole, what made the measurements of wave front tilts feasible only in the radial axial cross sections of the beam with a separated-out ring aperture. In the other modification, a mask with 25 round holes was used as a diaphragm. The mask fully overlapped the beam aperture. To provide for the limiting sensitivity of measurements of the local tilts of wave front subapertures and to exclude mutual overlapping of beams focused by the objective, an array of optical wedges was used. The optical wedges directed the beams toward the objective at different angles.

To determine aberrations of the optical path during laser generation series, the values of the maximum change of the mutual inclination angle (θ^*_{max}) of radial symmetric (by the position on the ring subaperture in the first modification of the measurement technique) wave front areas of the sensing radiation in the vertical and horizontal planes were used, as well as (for the second modification) the values of the maximum change of the angle θ_{max} of mutual inclination of wave front subapertures of the sensing radiation in the horizontal and vertical planes.

Table 1. Coefficients of aerosol extinction and scattering at the wavelength of 10.6 μm

Temperature, °C	10…11	17…19	15…18	14…18	15…18	13…14
Humidity, %	70…80	52…63	57…70	70…90	82…91	57…90
S_m, km	9…14	7…13	7…13	5…13	12	9…13
$K_{sc\ exp}$, 1/km		$2.5 \cdot 10^{-4}$	$3 \cdot 10^{-3}$	$1.6 \cdot 10^{-3}$		$4.0 \cdot 10^{-4}$
$K_{sc\ calc}$, 1/km		$5 \cdot 10^{-3}$	$3.2 \cdot 10^{-3}$	$3 \cdot 10^{-3}$		$1.0 \cdot 10^{-3}$
$K_{ext\ exp}$, 1/km	0.067	0.029	0.02	0.1	0.021	0.045
$K_{ext\ calc}$ 1/km	0.03	0.01	0.016	0.067	0.012	0.015

Table 2

f, Hz	P_r, W/cm^2	ΣE_r, kJ	φ	k_{abs}	γ	V, m/s	$V_\perp$, m/s	$\theta_{x\max}$, 10^{-4} rad	$\theta_{y\max}$, 10^{-4} rad
50	7.8	25.3	0.54	0.46	7°	3.4	0.5	1.5	1.9
50	8.1	17.5	0.42	0.56	107°	1.4	1.3	2.3	0
50	9.4	19.4	0.52	0.43	17°	3.3	1.0	1.5	1.1
50	9.4	20	0.38	0.48	107°	0.8	0.8	1.5	1.5
100	15.9	34.8	0.34	0.43	102°	1.4	1.4	3.8	4.5
100	18.9	35.9	0.36	0.4	287°	1.6	1.5	3.8	3.3
200	19.7	21.0	0.5	0.39	27°	4.5	2.0	3.4	5.3
200	23.0	41.7	0.33	0.49	107°	0.8	0.8	7.0	6.4

Note. f is the pulse repetition frequency; P_r is the mean power density of the radiation in the beginning of the path; ΣE_r is the total energy of laser pulses in the series; φ is the series mean energy emitted into the solid angle of $6 \cdot 10^{-4}$ rad; k_{abs} is the absorption coefficient of the path (L = 2.81 km); γ is the orientation of the wind direction with respect to the direction of the optical path; V is the wind velocity during the series; $V_\perp$ is the transverse component of the wind velocity with respect to the atmospheric path; $\theta_{x\max}$ is the maximum relative angular aberration of the optical path in the horizontal plane; $\theta_{y\max}$ is the maximum relative angular aberration of the optical path in the vertical plane.

Table 2 presents the measured values of θ_{max} along with the main experimental conditions. These data were obtained in summer experiments with the laser operated along the path with the length L = 2.81 km. The laser generation series lasted from 1 to 3 s. In determination of θ_{max}, the results of measurements of thermal deformations of optical elements set in the path of the high-power beam were taken into account. In summer experiments with the limiting power ~ 30 kW and the atmospheric path with the length L = 2.7 km, angular aberrations θ_{max} achieved $6 - 7 \cdot 10^{-4}$ rad. In winter experiments with the power ~ 20 kW and the paths of 0.9 – 2.1 km long, $\theta_{max} \approx 3 \cdot 10^{-4}$ rad. The obtained data indicate that θ_{max} directly depends on the total energy of laser radiation having passed the path and on the pulse repetition frequency. At the same time, (probably, because of the limited volume of experimental data) we failed to find the dependence of θ_{max} on other experimental conditions.

Nevertheless, the obtained data agree with the estimates of typical values of the power density of laser radiation at which the effect of thermal blooming manifests itself in the atmosphere.[17] For summer conditions and at the cross wind of 2 m/s at a 3-km long atmospheric path, the maximum possible radiation power at the path's entrance should be no higher than 15 W/cm^2 for the effect of thermal blooming not to manifest itself.

To estimate the influence of thermal blooming on the radiation intensity distribution over the aperture of the focused beam, the latter is to be focused onto a remote object provided that the radiation power density at the path's entrance is lower than 15 W/cm^2, it was proposed in Ref. 3 to use the normalized coefficient of radiation delivery within a small solid angle

$$K_\varphi = E_{d\varphi}/(T\, E_{0\varphi}), \qquad (2)$$

where $E_{d\varphi}$ is the maximum energy delivered per pulse into the receiving aperture with the angular size φ; $E_{0\varphi}$ is the radiant energy in the same laser pulse and within the same angle, but at the path's entrance; T is the transmission coefficient of the atmospheric path.

It was found that in this case the delivery coefficient is a function of the nonlinear phase change $\Delta\varphi_{nl}$ calculated only for the area of beam caustic on the path:

$$\Delta\varphi_{nl} = 2\pi \frac{\partial n}{\partial T} \alpha\, l_S\, P_S/(\lambda\rho\, V_\perp\, d_S\, C_P), \qquad (3)$$

where d_S is the integrated over the series of pulses beam diameter in caustic with due regard for the beam wandering; P_S is the power of radiation delivered to the area of caustic; l_S is the caustic length; α is the absorption coefficient of the atmosphere; $V_\perp$ is the cross component of the wind velocity.

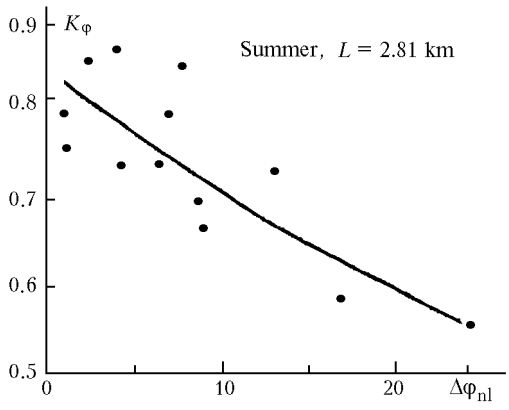

Fig. 2. Experimental dependence of the normalized coefficient of laser energy delivery K_φ on the nonlinear phase change $\Delta\varphi_{nl}$ in the summer cycle of experiments on propagation of radiation of repetitively pulsed CO_2 laser.

Figure 2 illustrates the experimental dependence of the normalized coefficient of delivery of laser energy K_φ on the value of the nonlinear phase change $\Delta\varphi_{nl}$ obtained in the summer cycle of experiments.[3] The solid curve in Fig. 2 is the exponential approximation of the experimental data obtained by the method of least squares. It is seen that already as the power density of the laser beam in the area of caustic was $20-40$ W/cm^2 in the experiments, the efficiency of radiation delivery in the small (less than the diffraction-limited one) spatial angle fell down significantly.

Figure 2 shows only that experimental data, for which the state of the atmospheric path was characterized by a relatively low level of turbulent perturbations. At a strong turbulence (that is, at $C_n^2 > 2 \cdot 10^{-14}$ m$^{-2/3}$), we did not observe a correlation between the above parameters because of the strong (up to speckling) distortions of the radiation intensity distribution over the laser beam aperture.

As the experiments showed,[2] the atmospheric turbulence is the main factor, which significantly restricts the efficiency of precise delivery of CO_2-laser radiation with power up to 35 kW along the near-ground atmospheric paths. For analysis of these restrictions we considered such characteristics of the beam as the variance of random shifts of the energy centroid of the laser beam σ_c^2 and the mean intensity at the beam axis after it passed through a turbulent atmospheric layer.

Figure 3 shows the dependence of these parameters on the structure constant of fluctuations of the refractive index C_n^2. These data were obtained in the same summer cycle of experiments along the atmospheric path 2.81 km long.[2] The experimental data in Fig. 3 corresponds to the laser operation series no less than 1.5 s in duration. It is seen that the marked influence of the atmospheric turbulence both on the stability of the spatial position of the laser beam and on the mean radiation intensity manifests itself at $C_n^2 > 10^{-14}$ m$^{-2/3}$ (under the conditions of the experiment).

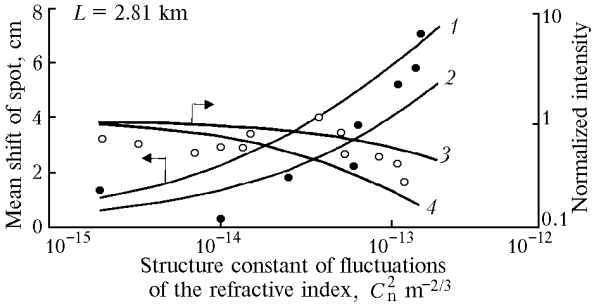

Fig. 3. Influence of the atmospheric turbulence on the value of random shifts and the intensity at the axis of the beam of repetitively pulsed CO_2 laser for a 2.81-km long near-ground atmospheric path.

In this case, random shifts of the energy centroid of the beam become comparable with its diffraction-limited size. It should be noted that in the experiments the radius of the diffraction-limited beam focused at the distance of 2.81 km was equal to 7 cm.

The variance of random shifts of the laser beam with the Gaussian intensity distribution is described by the following equations[18]:

$$\delta_c^2 = (8/9)\, \delta_{co}^2\, \delta_L^2,$$
$$\delta_{co}^2 = 1.52\, C_n^2\, L^3\, a^{-1/3}, \qquad (4)$$
$$\delta_L^2 = 3a^{1/3} \int_0^1 (1-x)^2 \times$$
$$\times \{a_{eff}^{-1/3}\,(xL) - [a_{eff}^2(xL) + a^2 b]^{-1/6}\}\, dx.$$

Here b is the outer scale of turbulence; a_{eff} is the effective beam radius in the turbulent atmosphere

$$a_{eff}^2 = (a^2/\Omega^2)\,[1 + a^2/a_k^2 + (4/3)\, a^2/\rho^2], \qquad (5)$$

where $a_k = (1.45\, C_n^2\, k^2\, L)^{-3/5}$ is the coherence length of the field of the plane wave; $\Omega = k\, a^2/L$ is the Fresnel number of the transmitting aperture; a is the initial beam radius.

In particular, Fig. 3 shows the calculated results on the variance of random shifts for beams with the initial wave front curvature corresponding to either the diffraction divergence of the beam ($\lambda/2a$ – curve *1*) or four times higher divergence (curve *2*), i.e., that observed in the experiments. In this case, the parameter b characterizing the outer scale of turbulence was calculated by the equation $b = 2\,(H/5\pi a)^2$, in which H is the mean altitude of the path above the ground.[18]

Comparing the experimental and calculated data, we can conclude that the initial divergence of the laser beam (i.e., curvature of its wave front) only slightly affects the variance of random spatial walks of the beam in a strongly turbulent atmosphere.

Figure 3 also shows the calculated values of the mean normalized intensity for Gaussian beams with the initial radius two and three times less than the original one (curves *3* and *4*, respectively). For calculations we used the analytical equations from Ref. 20, which describe the distribution of the mean intensity in the cross section of the Gauss laser beam in the turbulent atmosphere:

$$\langle I(R)\rangle = \frac{P}{\pi a_d^2} \int_0^\infty J_0(2R\sqrt{t/a_d}) \times$$
$$\times \exp\left[-t - \frac{1}{2} D_S\,(2a/g_1)\, t^{5/6}\right] dt, \qquad (6)$$

where P is the radiation power; $a_d = Lg_1/Ka$ is the beam radius in the homogeneous medium; $J_0(z)$ is the zero-order Bessel function. For the focused beam $g_1^2 = 1 + a^2/a_k^2$.

It is seen that the initial divergence of laser radiation strongly affects the mean intensity at the beam axis in the turbulent atmosphere. At a weak turbulence, the improvement of the beam quality at the path's entrance allows the radiation intensity at a given point of a remote receiver to be increased, however at a

strong atmospheric turbulence the quality of the laser beam practically does not influence the axial brightness of radiation at the receiver.

From the practical point of view, it is important to determine such optimal combination of the parameters of a laser source and a telescope system, with which it is possible to avoid compensating for the influence of the atmosphere on the accuracy of radiation delivery.

Figure 4 shows the calculated dependence of the mean intensity at the beam axis on the aperture of the primary mirror of a forming telescope and the initial beam divergence. The calculation was performed with the use of Eq. (6) for two lengths of the atmospheric path (1 and 3 km) and for the altitude of 3–4 m above the ground, i.e., under the same conditions as the experimental ones. From the comparison of the curves in Figs. 4*a* and *b* it is clear that at a long path (longer than 3 km) and at strong turbulence ($C_n^2 > 1 \cdot 10^{-13}$ m$^{-2/3}$) the improvement of the beam divergence from four diffraction angles to one is tantamount to the increase of the exit aperture of the telescope up to 0.6–0.8 m. At a weak turbulence, the intensity at the beam axis can be significantly increased by increasing the exit aperture of the telescope, but it is impossible at strong turbulence.

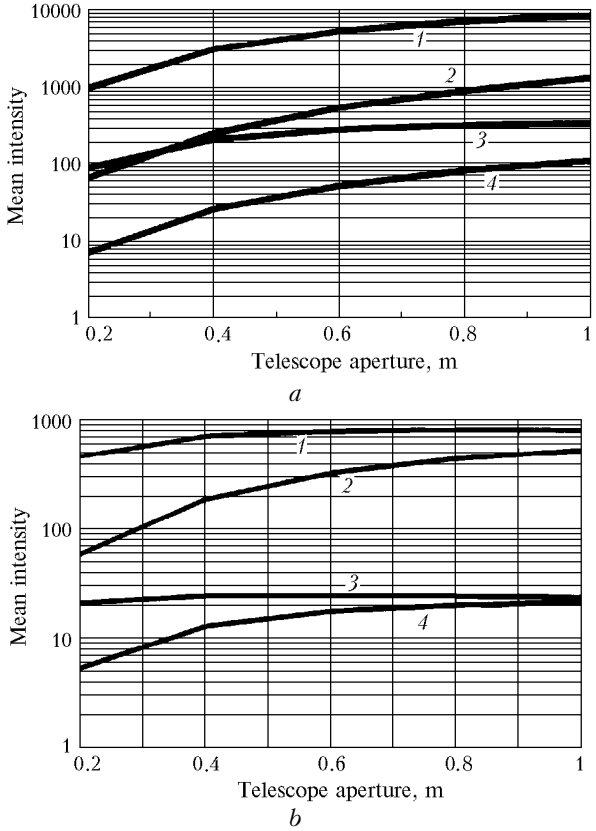

Fig. 4. Dependence of mean intensity at the beam axis in the turbulent atmosphere on the aperture of a forming optical system. The path length is 1000 m (*1*, *2*) and 3000 m (*3*, *4*). The radiation divergence is diffraction one (*1*, *3*) and four times wider (*2*, *4*). $C_n^2 = 1 \cdot 10^{-14}$ m$^{-2/3}$ (*a*) and $C_n^2 = 1 \cdot 10^{-13}$ m$^{-2/3}$ (*b*).

Thus, experimental results and numerical estimates under the considered conditions indicate the weak dependence of the spot wandering on the radiation wavelength, divergence, and the initial size of the laser beam. So, to optimize the radiation delivery in the turbulent atmosphere, specialized algorithms should be developed to control over the laser beam.

An original algorithm for stabilization of the position of a high-power laser beam has been proposed at the R&D Institute for Laser Physics (St. Petersburg).[20] It is based on stabilization of the position of the point of maximum intensity in the beam cross section, rather than the beam centroid. The brightest speckle in the intensity distribution over the beam aperture is such a point for the beam passing through the turbulent atmosphere. The method is based on active search for the optimal direction of a high-power laser beam with the help of a probing radiation at the same wavelength.

The main requirement to the implementation of this algorithm is coincidence, to a high accuracy, of the wave fronts of the probing and high-power beams. The control criterion is given by the level of power of the reflected signal of the trial radiation. The high-power laser pulse is generated when the level of the trial signal is maximum. If optical distortions at the beam propagation path are frozen for the time of double passage of the trial beam, then we can expect that they will be partially compensated due to stabilization of the position of the high-power beam at the given point of the receiver.

To provide for coincidence of the wave fronts of the probing and high-power beams, in Ref. 20 the optical scheme of the master oscillator of the probing radiation was proposed to be the so-called scheme of a two-mode oscillator capable of operating in both the continuous-wave and repetitively pulsed modes, and the high-power laser was proposed to be assembled using the scheme of a two-passage amplifier with an OWF mirror. Obviously, the accuracy of coincidence of the wave fronts in this case is mostly determined by the accuracy of OWF compensation of optical inhomogeneities in the active medium of the high-power laser.

This algorithm was checked with the use of an electroionization CO_2 laser and an interior (laboratory) atmospheric path 230 m long. The results of this check are presented in Ref. 4. The atmospheric turbulence along the laboratory path was simulated by use of extra aberrators of a laser beam. The aberrators introduced both long-scale distortions of a beam (in the form of dynamic deflections of the beam within $\pm \lambda/D$) and small-scale ones simulating beam speckling. As this took place, the character and dynamics of laser beam changes at the end of the path simulated the behavior of a laser beam at an actual 3-km long near-ground atmospheric path (with $C_n^2 \sim 10^{-13}$ m$^{-2/3}$).

Table 3 gives the main results obtained in the check of the algorithm of "bright speckle" under different conditions of beam propagation along the

atmospheric path. Two parameters are used to make up a criterion of the algorithm efficiency: the parameter of radiation delivery η and the angular deviation of the bright speckle from a given position ($\Delta\theta$). The parameter η was determined as the ratio of the laser pulse energy falling within the aperture with the angular size 0.35 λ/D with allowance made for the loss along the path to the energy contained within the same angle but at the amplifier output.

Table 3. Results of the check of the bright speckle algorithm along the laboratory path

IM1	IM2	Laser mode	Without algorithm		With algorithm	
			η (λ/D)	$\Delta\theta$ (λ/D)	η (λ/D)	$\Delta\theta$ (λ/D)
+	–	1 Hz	0.16	0.92	0.42	0.35
+	–	20 Hz	0.13	1.69	0.38	0.40
+	+	1 Hz	0.06	1.88	0.22	0.31
+	+	20 Hz	0.04	1.89	0.17	0.33

When only the aberrator (IM1) introducing large-scale aberrations in the laser beam was turned on, the run of the algorithm led to a 3 to 7 times increase of the series mean efficiency of radiation delivery. The maximum value of η in this case was 0.48. When a simulator of small-scale aberrations (IM2) was turned on, the value of η did not exceed 0.25 even if the central maximum fell within the aperture of the remote receiver with a sufficient accuracy. The decrease of the delivered energy in this case is caused by the decrease of the energy density in the central maximum of the beam intensity distribution because of the appearance of extra lateral maxima (speckles). Nevertheless, the run of the stabilization algorithm also led to a 3 to 4 times increase of the efficiency of radiation delivery and to the decrease of the mean deviation of the bright speckle from a given position ($\Delta\theta$) up to 0.3 λ/D.

As analysis of the experiments showed, stabilization of the spatial position of the high-power beam with the use of the algorithm of bright speckle was restricted, first of all, by replacement of the OWF mirror with a corner-cube retroreflector.

To determine the required accuracy with which the wave fronts of the high-power and probing beams coincide in the case that these beams pass through the turbulent atmosphere, let us consider in a more detail the influence of such factors as different positions of the beam axes and different curvature of their wave fronts at the path's entrance on decorrelation of speckle patterns of both beams.

The correlation function of speckles in the observation plane can be a measure of decorrelation of speckle patterns. As the scanning coherent radiation passes through a turbulent layer in the atmosphere, a dynamical speckle pattern arises, i.e., the spatial structure of the scattered radiation varies with time depending on the scanning angle.

To relate the fields of the beam with the scanning angle θ, let us consider a fixed coordinate system (x, y, z) (Fig. 5), in which the axis z is normal to the observation plane; θ is the angle between the normal to the observation plane (axis z) and the direction of the beam propagation (axis z'). Assuming that scanning occurs near the normal to the surface ($\theta \ll \pi/2$; $\sin\theta \cong \theta$; $\cos\theta \cong 1$) and the radiation source is in the plane $z = 0$, we can write the field in the plane *1* ($z = 0$) retaining only the terms of the first order of smallness in terms of the angle θ:

$$E_1(\mathbf{x}, \theta) = E_0 \exp\{-(1/w^2)(x^2 + y^2) - ikx\theta - [ik/(2\pi)](x^2 + y^2)\}, \quad (7)$$

$\mathbf{x} = (x, y)$, the term $i\varphi_0$ (initial phase) in braces is omitted.

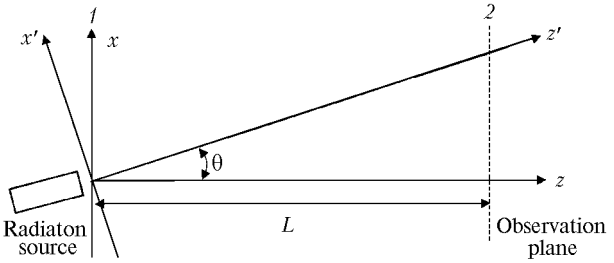

Fig. 5. Optical arrangement used in calculating correlation functions of dynamical spatial structure of scattered radiation.

The field of a light wave that passed through the turbulent layer and achieved the observation plane can be written based on the generalized Huygens–Kirchhoff method[21] in the Fresnel diffraction approximation:

$$E_2(\mathbf{x}, \theta) = \frac{ie^{-ikL}}{\lambda L} \iint_{-\infty}^{+\infty} E_1(\mathbf{x}_1, \theta) \exp\left\{-\frac{ik}{2L} \times [(x - x_1)^2 + (y - y_1)^2] + \Psi(\mathbf{x}, L; \mathbf{x}_1, 0)\right\} dx_1\, dy_1, \quad (8)$$

where $\Psi(\mathbf{x}, L; \mathbf{x}_1, 0)$ determines the random change of the complex phase as the spherical wave propagates from the point $(\mathbf{x}, 0)$ to the point $(\mathbf{x}_1, L)$.

The correlation function of the light field in the observation plane (plane *2* in Fig. 5) for the beams propagating through the turbulent layer at different angles θ_1 and θ_2 with respect to the normal to the observation plane can be written as:

$$C(\mathbf{x}, \theta_1, \theta_2) = \langle E_2(\mathbf{x}, \theta_1) E_2^*(\mathbf{x}, \theta_2)\rangle = \frac{1}{(\lambda L)^2} \iint_{-\infty}^{+\infty} E_1(\mathbf{x}_1, \theta_1) E_2^*(\mathbf{x}_2, \theta_2) \times \langle \exp\{\Psi(\mathbf{x}, L; \mathbf{x}_1, 0) + \Psi^*(\mathbf{x}, L; \mathbf{x}_2, 0)\}\rangle \times \exp\left\{-\frac{ik}{2L}[(x - x_1)^2 + (y - y_1)^2 - (x - x_2)^2 - (y - y_2)^2]\right\} dx_1\, dy_1\, dx_2\, dy_2. \quad (9)$$

In the case of the normal distribution of the change of the complex phase Ψ, the moment of the vector e^{Ψ} can be presented as[21]:

$$<\exp [\Psi(\mathbf{x}, L; \mathbf{x}_1, 0) + \Psi^*(\mathbf{x}, L; \mathbf{x}_2, 0)]> = \\ = \exp \{-|\mathbf{x}_1 - \mathbf{x}_2|^{5/3}/\alpha_0\}, \quad (10)$$

where $\alpha_0 = (0.545625\, C_n^2\, Lk^2)^{-1}$, C_n^2 is the structure constant of the atmospheric refractive index.

Equation (10) was derived based on the Kolmogorov model for the spectrum of fluctuations of the refractive index of the turbulent atmosphere. In the general case, Eq. (9) cannot be integrated analytically with the allowance for Eq. (10). Therefore, sometimes the approximate substitution is used in the equations for statistical moments[21]:

$$\exp (-\mathbf{x}^{5/3}/\alpha_0) \to \exp (-\mathbf{x}^2/\alpha_0^{6/5}). \quad (11)$$

Denote $l_0^2 = (0.545625\, C_n^2\, Lk^2)^{-6/5}$.

Upon integration of Eq. (9) with the allowance for Eqs. (10) and (11) and substitution of variables, we obtain:

$$C(\mathbf{x}, \theta_1, \theta_2) = [E_0^2\, \pi^2\, w^2/(\lambda^2\, L^2\, 2Q_1)] \times \\ \times \exp (-k^2 w^2 \Delta_\theta/8) \times \\ \times \exp \{-k^2/4Q_1\, [(x^2 + y^2)/L^2 - xS_\theta/L + S_\theta^2/4 - \\ - w^4/16L^2\, \Delta_\theta^2\, (1 + L/\rho)^2 + (ik^3 w^2)/2L \times \\ \times (x/L - S_\theta/2)\, \Delta_\theta\, (1 + L/\rho)]\}. \quad (12)$$

Here

$$\Delta_\theta = \theta_1 + \theta_2; \qquad S_\theta = \theta_1 - \theta_2;$$

$$Q_1 = \frac{1}{2w^2} + \frac{1}{l_0^2} + \frac{k^2\, w^2}{8L^2}\left(1 + \frac{L}{\rho}\right)^2. \quad (13)$$

In accordance with the Eqs. (9) and (10), for the absolute value of the normalized correlation function we have

$$\gamma(\Delta_\theta) = \exp \{-k^2 w^2/(8l_0^2\, Q_1)\, \Delta_\theta^2\}. \quad (14)$$

Figure 6 shows the dependence of the normalized correlation function on the difference of the scanning angles Δ_θ. Curve *a* in Fig. 6 was calculated for the laboratory conditions: the path with the length $L = 240$ m, parameters of the initial beams $w = 65$ mm, $\rho = -240$ m (the radiation is focused to the observation plane); the level of turbulence on the path corresponds to $C_n^2 = 2 \cdot 10^{-12}$ m$^{-2/3}$, $\beta^2 = 0.309$ ($\beta^2 = 1.23\, C_n^2\, k^{7/6} \times L^{11/6}$ is the parameter characterizing fluctuations of the plane wave). The parameter C_n^2 and, correspondingly, β^2 were chosen so that the intensity distribution, averaged over the ensemble of realizations, in the observation plane was closest to similar distribution in the case when turbulence is simulated by a phase screen with the parameters presented in Ref. 3. It is seen from Fig. 6*a* that the width of the normalized correlation function at the level of e^{-1} is equal to 10^{-4} rad; at the level of 0.9 it is about $5 \cdot 10^{-5}$ rad. Thus, significant decorrelation can occur when the scanning angle is changed by 10^{-4} rad (i.e., when the angles of inclination of the scanning and the high-power beams differ by this value). If it is needed to reproduce the speckle pattern with higher accuracy, for example, for the correlation to be $\gamma(\mathbf{x}, \theta_1, \theta_2) \approx 0.95 - 0.9$, then the difference between these angles should be within $(1 - 3) \cdot 10^{-5}$ rad.

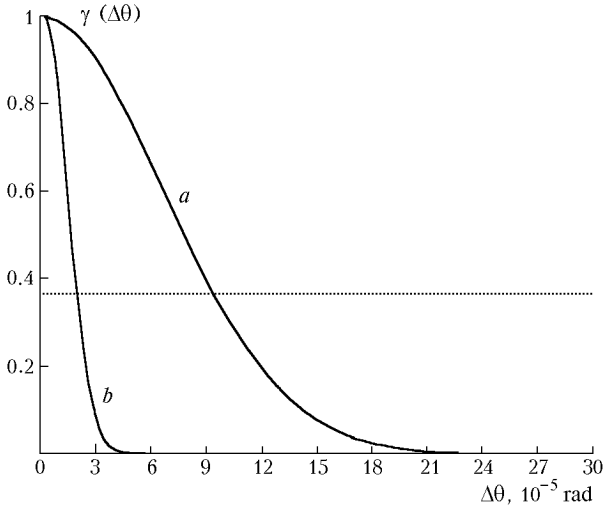

Fig. 6. Normalized correlation function of radiation in the observation plane for Gaussian beams that passed through the turbulent layer at different angles θ_1 and θ_2 with respect to the observation plane ($\Delta_\theta = \theta_1 - \theta_2$): $L = 240$ m, $w = 65$ mm, $\rho = -240$ m, $C_n^2 = 2 \cdot 10^{-12}$ m$^{-2/3}$, $\beta^2 = 0.309$ (*a*); $L = 3$ km, $\rho = -3$ km, $w = 25$ cm, $C_n^2 = 2 \cdot 10^{-13}$ m$^{-2/3}$, $\beta^2 = 1.584$ (*b*).

The degree of correlation significantly depends on the beam path length and the level of turbulence at the path, and in the general case it is determined by the parameter β^2. Figure 6*b* shows the corresponding data calculated for the path with the length $L = 3$ km for $\rho = -3$ km and $w = 25$ cm with the parameters of turbulence $C_n^2 = 2 \cdot 10^{-13}$ m$^{-2/3}$, that is, $\beta^2 = 1.584$. It is seen that in this case the requirements to the coincidence of the beams relative to the tilts of their wave fronts are more strict, namely, for the correlation level of e^{-1} they must coincide accurate to $\sim 2 \cdot 10^{-5}$ rad, and for the level of 0.9 they must coincide accurate to $5 \cdot 10^{-6}$ rad. That is, the accuracy should be an order of magnitude higher than that achieved on the model laboratory path.

The requirements to coincidence, in the observation plane, of the wave front curvature of the beams passed through the turbulent atmospheric layer can be determined in a similar way. In this case, the correlation function in the observation plane for the Gaussian beams with different radii of curvature of the wave fronts at the turbulent medium entrance, ρ_1 and ρ_2, but with the same beam radius w at the level of intensity of e^{-2} can be determined as

$$C(\mathbf{x}, \rho_1, \rho_2) = \langle E_2(\mathbf{x}, \rho_1)\, E_2^*(\mathbf{x}, \rho_2)\rangle. \quad (15)$$

Similarly to the above consideration [by substituting Eq. (8) into Eq. (15), using Eq. (10) in the approximation (11), and integrating], we have for the correlation function that

$$C(\mathbf{x}, \rho_1, \rho_2) = E_0^2\, \pi^2 \,/\, \lambda^2\, L^2 \left(\frac{2}{w^2} + \frac{ik}{2\Delta_\rho}\right) Q_2 \times$$
$$\times \exp\{k^2\,(x^2 + y^2)/(4L^2\, Q_2)\}, \quad (16)$$

where

$$Q_2 = \frac{1}{2w^2} + \frac{ik}{8\Delta_\rho} + \frac{1}{l_0^2} + \frac{k^2}{16 S_\rho\,[(2/w^2) + ik/(2\Delta_\rho)]};$$

$$\frac{1}{\Delta_\rho} = \frac{1}{\rho_1} - \frac{1}{\rho_2}; \quad \frac{1}{S_\rho} = \frac{1}{\rho_1} + \frac{1}{\rho_2} + \frac{2}{L}.$$

Figure 7 shows the plots of the normalized correlation function

$$c(\rho_1, \rho_2) = |C(\mathbf{x}, \rho_1, \rho_2)/C(\mathbf{x}, \rho_1, \rho_1)|, \quad (17)$$

calculated at the origin of coordinate in the observation plane $x = 0$, $y = 0$.

The dependence of the correlation function (curve in Fig. 7*a*) on the value of ρ_2 at a fixed value of ρ_1 was calculated for the laboratory conditions: the path with the length $L = 240$ m, the beam radius $w = 65$ mm at the level of intensity of e^{-2}, $\rho_1 = -240$ m (the radiation is focused onto the observation plane); the level of turbulence on the path corresponds to $C_n^2 = 2 \cdot 10^{-12}$ m$^{-2/3}$, $\beta^2 = 0.309$. Figure 7*b* shows similar dependence corresponding to the path with $L = 3$ km, i.e., $\rho_1 = -3$ km, $w = 25$ cm with the turbulence parameters $C_n^2 = 2 \cdot 10^{-13}$ m$^{-2/3}$, $\beta^2 = 1.584$.

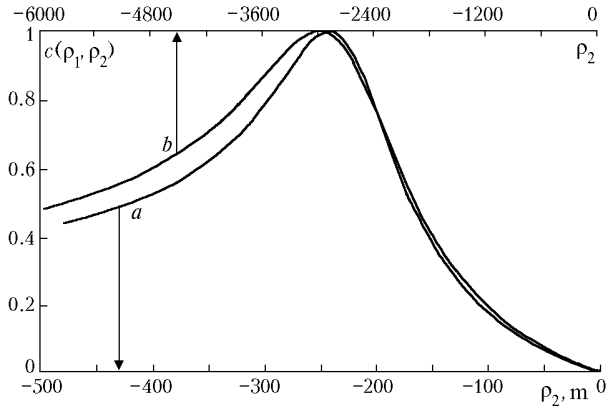

Fig. 7. Normalized correlation function of radiation for beams with different curvature lengths of wave front ρ_1 and ρ_2 upon propagation through the turbulent layer: $\rho_1 = -240$ m, $x = 0$, $y = 0$ (*a*); $\rho_1 = -3000$ m; $x = 0$, $y = 0$ (*b*).

As is seen from the plots, the requirements to coincidence of the curvature of wave fronts of the scanning and high-power beams are less strict. The normalized correlation function decays no lower than 0.9 when the wave fronts coincide accurate to ± 10%. As calculations show, the requirements to the quality of the OWF mirror which should be used in a double-pass amplifier are rather high.

Conclusion

Based on analysis of the experimental results on passage of the radiation of a high-power repetitively pulsed CO_2 laser through the atmosphere and the numerical estimates, the peculiarities significant for radiation delivery to remote objects have been revealed in interaction of such radiation with the atmosphere. Direct measurement of the optical quality of the atmospheric path of the high-power beam confirms the appearance of thermal distortions of this path at the radiation power density at the path's entrance no lower than 15 W/cm^2. At the power density of the laser beam of 20 – 40 W/cm^2 in the area of caustic, the efficiency of radiation delivery into a small (less than the diffraction size) spatial angle decreases markedly. Under atmospheric conditions, the effect of thermal blooming is partially screened by the atmospheric turbulence and, on the whole, only slightly affects the efficiency of radiation delivery. It has been shown that to estimate this effect correctly, one needs to correct the values of the real and imaginary parts of the refractive index of atmospheric aerosols at the wavelength of 10.6 μm, which are usually used in calculations of the absorbed laser energy. (The problems of nonlinear extinction in water aerosol were considered in detail in Refs. 22 and 23.)

The efficiency of transfer of high-power radiation through the atmosphere is markedly affected by such factors as insufficient monochromaticity of the laser line and collisional shifts of the center of the laser line and the center of the absorption line of the atmospheric carbon dioxide.

The atmospheric turbulence significantly limits the efficiency of delivery of CO_2-laser radiation with power up to 30 kW along the near-ground atmospheric paths. The experimental results and numerical estimates under the considered conditions are indicative of the weak dependence of spot walks on the divergence and the initial size of the laser beam.

As analysis shows, the radiation intensity at the beam axis cannot be significantly improved by increasing the exit aperture of the forming telescope under conditions of a strong turbulence ($C_n^2 > 10^{-13}$ m$^{-2/3}$), a specialized algorithm for controlling the laser beam should be developed for optimizing the radiation delivery in the turbulent atmosphere. Capabilities of one such algorithm – the algorithm of bright speckle – have been considered as applied to stabilization of the beam position at a remote receiver, and the requirements to the accuracy of coincidence of the wave fronts of the probing and high-power laser beams have been determined to provide for efficient operation of the algorithm.

Acknowledgments

The authors are indebted to N.F. Borisova, L.A. Glushchenko, and V.L. Okulov for their help in numerical calculations.

References

1. P. Carrick, F. Mead, and L. Myrabo, Optics and Photonics News **42**, 23–25 (1999).
2. A.A. Ageichik, I.M. Belousova, D.A. Goryachkin, et al., Opt. Zh., No. 11, 5–14 (1999).
3. A.A. Ageichik, D.A. Goryachkin, O.G. Kotyaev, et al., Opt. Zh., No. 11, 15–22 (1999).
4. A.A. Ageichik, M.P. Bogdanov, V.V. Valuev, et al., Opt. Zh., No. 11, 23–33 (1999).
5. I.M. Belousova, I.V. Glukhikh, A.V. Dutov, et al., Kvant. Elektron. **13**, No. 2, 260–265 (1986).
6. Yu.G. Agalakov, M.O. Bulanin, V.V. Bertsev, et al., Opt. Spektrosk. **58**, No. 3, 493–495 (1985).
7. P. Aras, E. Arie, C. Boulet, et al., J. Chem. Phys. **73**, No. 10, 5383–5384.
8. N.F. Borisova, E.S. Bukova, V.M. Osipov, and V.V. Tsukanov, Atm. Opt. **4**, No. 1, 49–54 (1991).
9. L.S. Vasilenko, M.N. Skvortsov, V.P. Chebotaev, et al., Opt. Spektrosk. **32**, No. 6, 1123–1129 (1972).
10. K.L. Sooho, Ch. Freed, J.E. Thomas, et al., IEEE J. of Quant. Electron. **QE21**, No. 8, 1159–1171 (1985).
11. N.F. Borisova, V.M. Osipov, and N.I. Pavlov, Kvant. Elektron. **12**, No. 12, 2505–2507 (1985).
12. V.M. Osipov, N.F. Borisova, O.M. Galantseva, et al., Opt. Zh., No. 11, 39–46 (1999).
13. V.L. Okulov, Yu.A. Rezunkov, P.V. Sidorovskii, et al., Opt. Zh., No. 11, 39–46 (1999).
14. *Atmosphere. Reference Book* (Gidrometeoizdat, Leningrad, 1991), 508 pp.
15. V.A. Filippov, A.S. Makarov, and V.P. Ivanov, Dokl. Akad. Nauk SSSR **265**, No. 6, 1353–1356 (1982).
16. S.D. Andreev, N.F. Borisova, L.S. Ivlev, et al., in: *Proceedings of the II International Conference on Natural and Anthropogenic Aerosols* (St.-Petersburg State University, St. Petersburg, 1999), pp. 19–20.
17. V.P. Lukin, *Atmospheric Adaptive Optics* (Nauka, Novosibirsk, 1986), 248 pp.
18. V.L. Mironov, *Laser Beam Propagation through the Turbulent Atmosphere* (Nauka, Novosibirsk, 1981), 246 pp.
19. A.S. Gurvich, A.I. Kon, V.L. Mironov, et al., *Laser Radiation in the Turbulent Atmosphere* (Nauka, Moscow, 1976), 280 pp.
20. V.E. Sherstobitov, V.I. Kuprenyuk, D.A. Goryachkin, et al., Proc. SPIE **3684**, 51 (1999).
21. V.E. Zuev, V.A. Banakh, and V.V. Pokasov, *Optics of the Turbulent Atmosphere* (Gidrometeoizdat, Leningrad, 1988), 270 pp.
22. V.A. Pogodaev, Atmos. Oceanic Opt. **6**, No. 4, 211–213 (1993).
23. N.N. Bochkarev, Yu.E. Geints, A.A. Zemlyanov, et al., Atmos. Oceanic Opt. **11**, No. 7, 602–608 (1998).